Eigenfunction-expansion method for solving the quantum-wire problem: Formulation

G. A. Baraff and D. Gershoni
AT&T Bell Laboratories, Murray Hill, New Jersey 07974
(Received 1 August 1990; revised manuscript received 15 October 1990)

We present a method of formulating the multiband-envelope-function equations for a quantum structure whose internal interfaces are perpendicular planes. The method can be used for quantum wells, quantum wires, or quantum dots (one-, two-, or three-dimensional confinement of the electronic wave function), as well as for periodic repetitions (superlattices) of these elementary structures. The technique used is expansion of the multiband envelope functions in a Fourier series for each of the coordinates x, y, and z. Special attention is paid to formulating interface-matching conditions that impose Hermiticity on the resulting systems of equations. This demand leads to the usual condition that the normal component of the current must be continuous across each internal interface. The method we have devised is similar to the one used by Altarelli for the quantum-well problem in that it leads to a secular equation that is solved by diagonalizing an energy-independent matrix. It differs in that here, the envelope functions are expanded in smooth continuous functions using the *same* expansion coefficients in all regions of the structure. Using this method, one can now calculate the optical absorption, its frequency, and polarization dependence, with the same amount of detail that has previously been possible only for confinement in one dimension, namely, in the quantum well and one-dimensional superlattice.

I. INTRODUCTION

Recent advances in semiconductor technology have made it possible to produce structures in which carriers are confined to one, two, or three dimensions in regions smaller than their mean free path. Properties of the carriers in such systems are probed by mainly using optical techniques. It is clearly of utmost importance to be able to calculate the electronic band structure and wave functions in such structures so as to make a comparison with the experiments.

There already exists extensive literature on how to do this for systems having one-dimensional confinement (quantum wells and superlattices). The need to extend this to higher dimensions is obvious. Three recent papers have made starts in this direction. In the first,[1] Gershoni *et al.* consider a quantum wire of rectangular geometry in which the confining potential $V(x,y)$ has one value in the confining region and other values in the outer regions. They used a one-band effective-mass model to describe the wave function.

In the second,[2] Citrin and Chang used a multiband-envelope-function wave function (valence bands only) to calculate properties of structures much like those studied by Gershoni *et al.* They simplified the problem by taking certain material parameters to be uniform throughout the entire structure. This bypassed the need for incorporating slope discontinuities of the envelope functions at internal interfaces. There are certainly computational advantages in doing this in cases where it is a good physical approximation. However, this approach leaves a gap in understanding how to proceed when the momentum matrix elements, for example, change from one region to the next. [Note: A recent paper by Citrin and Chang[3] uses the effective-bond-orbital model (EBOM)—a tight-binding approach in which the parameters are adjusted so as to reproduce the infinite-medium envelope-function approach—to overcome some of the shortcomings we cited with the earlier Citrin and Chang method. The EBOM method would seem to be a very useful and flexible one for problems of the sort being considered here.]

In the third paper,[4] Sercel and Vahalla also used a multiband-envelope-function formulation, but they let the material properties be cylindrically symmetric or spherically symmetric so as to produce two-dimensional or three-dimensional confinement. The enormous simplification this produces leads to analytic solutions that will undoubtedly be extremely valuable. Still, in many experimental situations, such as compositional modulation of the semiconductor properties along one direction with strain-induced modulation in an orthogonal direction, cylindrical or spherical symmetry is not useful as a simplifying assumption.

In this paper, we present a method for solving the multiband envelope functions in a one-, two-, or three-dimensional checkerboard geometry; that is, where the materials properties may change discontinuously across perpendicular planes, with special attention being given to the problem of matching functions at the boundaries. The technique used is Fourier-series expansion of the envelope functions.

It is convenient to use the quantum wire as the model for the derivation because the extension to three-dimensional variation or to one-dimensional variation is then trivial. Therefore, let us consider a three-dimensional semiconductor structure, uniform in one direction but composed of semiconductors whose properties, e.g., alloy composition and/or strain, vary in such a

way as to produce two-dimensional confinement of the electronic wave function. In the effective-mass approximation,[5] the wave function is expressed as the product of a slowly varying envelope function $F(r)$ and the cell periodic part of a zone-center Bloch wave $u(r)$. One has to solve a Schrödinger-like equation

$$\left[-\frac{\hbar^2}{2}\nabla\frac{1}{m(x,y)}\nabla+V(x,y)-E\right]F(r)=0\ , \tag{1.1}$$

where m is the effective mass, V is the potential, and where, for the time being, we have ignored the spin degree of freedom. Gershoni *et al.*[1] expressed the envelope function as a sum of eigenfunctions of the two-dimensional Laplacian operator, and thereby converted Eq. (1.1) into a matrix eigenvalue problem which was solved numerically. Even though both the mass and the potential may vary discontinuously from one region of the structure to another, this technique is valid, provided that the matrix elements contain terms (integrals over δ functions actually) that arise when the discontinuous $m(x,y)^{-1}$ is differentiated.

In studies of optical processes in quantum wells, wires, and dots (one-, two-, and three-dimensional confinement, respectively) the one-band effective-mass approximation is no longer adequate. One must instead consider a wave function of the form[5]

$$\psi(r)=\sum_{j=1}^{N}F_j(r)u_j(r)\ . \tag{1.2}$$

The sum goes over the N bands closest to the fundamental gap. Here, $u_j(r)$ is the cell-periodic part of a zone-center Bloch wave and $F_j(r)$ is the corresponding envelope function. The envelope functions are now governed by coupled differential equations and by interface continuity conditions (about which more will be said later). It is still possible to expand each envelope function as a sum of eigenfunctions of ∇^2. For the quantum-wire case, that expansion can have the form

$$F_j(r)=\sum_{m,n}F_j(m,n,p)\phi_m(x)\psi_n(y)e^{ipz}\ . \tag{1.3}$$

In such a situation, we can insert (1.3) into the coupled differential equations, make use of the interface boundary or continuity conditions, and arrive at a matrix eigenvalue equation whose general form is

$$\sum_{k,m',n'}H_{jk}(m,n;m'n';p)F_k(m',n',p)=E(p)F_j(m,n,p)\ . \tag{1.4}$$

If the spin degree of freedom is now restored, the indices j and k will be replaced by $j\sigma$ and $k\sigma'$, respectively, where σ and σ' can separately take on the values $\uparrow$ and $\downarrow$, referring to the two components of the electronic spin.

The extension from the one-band effective-mass situation to the multiband-envelope-function situation is a straightforward one, or should have been once the proper envelope-function interface-boundary continuity conditions had been formulated. However, we encountered difficulty on this point from the very outset, because there exist many derivations of envelope-function boundary conditions (several of which are completely unjustified) and these several lead to more than one interface prescription. We therefore studied the matching problem from different points of view. We ultimately found that if we insisted on boundary conditions which render the energy E real and the eigensolutions mutually orthogonal, we were led directly to the matching conditions that a majority of workers accept; namely, continuity of the unit-cell average of the normal component of the current. These are *not* the same boundary conditions that one obtains by blindly integrating the envelope functions across the interface unless those equations have first been put into a form specifically designed to guarantee Hermiticity. Not all workers have realized this and, for that reason, some of the boundary conditions appearing in the literature are simply wrong. Although our aim in undertaking the study had been to manipulate the equations in a mathematically rigorous way so as to obtain boundary conditions without relying on the physically well-motivated condition of current continuity, we failed to achieve this aim. Instead, we were still forced to go beyond the mathematics to the physics (namely, the demand for real energy and orthogonality) in order to establish boundary conditions. Insofar as we are thereby led back to the accepted interface condition, our understanding of interface matching has really not advanced past the state that Altarelli[6] described in 1986.

There already exists extensive literature on the envelope-matching problem and related topics. We have built on ideas already described in Refs. 7–23. Some of the cited papers have pointed out problems with earlier works. That literature is all accessible, and we shall not review it here.

The contents of the present paper are as follows. In Sec. II, we study a one-interface, spinless situation. In Sec. III, we specialize the geometry to the quantum wire, include spin, and obtain a prescription for constructing the elements of the matrix H. In Sec. IV, we give a "poor means derivation" of the results of Secs. II and III. This derivation is much easier to follow and apply than that of Secs. II and III but it contains steps whose *only* justification is that they reproduce results which have been obtained rigorously in the earlier sections. In the last section, Sec. V, we give a brief discussion of the advantages and disadvantages of this approach. The worker interested only in practical results can skip directly to Sec. IV, and from there, easily work out all the needed formulas.

II. A SIMPLE THREE-DIMENSIONAL CASE

Before going to the full detailed geometry of the quantum-wire situation treated in Sec. III, we consider the simplest three-dimensional case illustrated in Fig. 1. There is an inner region where the three-dimensional potential is that of semiconductor B. This is terminated by a closed surface S. Beyond this, there is a region where the potential is that of semiconductor A. That region in turn is terminated by the closed outer surface S_0. We

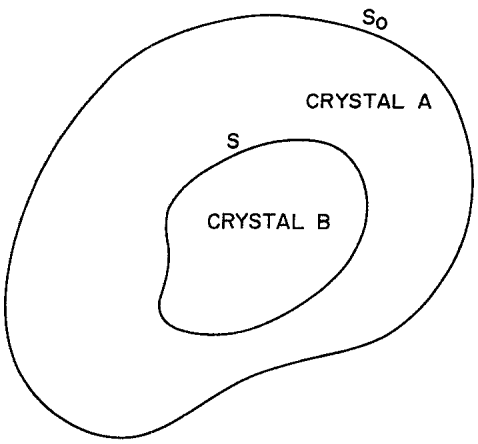

FIG. 1. Geometry used in the simplest three-dimensional situation where there is an inner region of semiconductor B surrounded by an outer region of semiconductor A.

want to solve the Schrödinger equation

$$H\psi(r)=[p^2/2m+V(r)]\psi(r)=E\Psi(r)$$

within the entire region bounded by S_0, subject to boundary conditions applied to ψ along S_0. We shall specify these outer boundary conditions later.

Representing the potential $V(r)$ as

$$V(r)=V^A(r), \quad r \text{ in } A$$

$$V(r)=V^B(r), \quad r \text{ in } B \ ,$$

where V^A and V^B are the perfect periodic potentials of crystals A or B is clearly an approximation. It neglects the change in potential caused by electronic reconstruction at the interface. However, numerical studies have shown this potential difference to be small for the situations of interest here,[24] and we ignore it, both because of its small size and also because including it would require information beyond that available at the level of the envelope-function approximation. Similarly, although there could be a long-range band-bending potential present, we ignore it also (it is simple to include it[5,6,10]) because our aim here is solely to study the discontinuities at the surface S.

The wave function is expanded in two sets of envelope functions, each multiplied by its associated zone-center Bloch wave,

$$\psi(r)=\sum_{j=1}^{\infty} F_j^A(r)u_j^A(r), \quad r \text{ in } A$$

$$\psi(r)=\sum_{j=1}^{\infty} F_j^B(r)u_j^B(r), \quad r \text{ in } B$$

where the Bloch waves are those appropriate to the infinite crystal A or B. Using such a composite representation (a functional expansion of one form in one region and another form in the other), the task of solving the Schrödinger equation comes down to obtaining equations for the envelope functions in each region separately, obtaining connection formulas to join the solutions in the two regions, and satisfying the outer boundary conditions. As we mentioned in the Introduction, we have not succeeded in formulating rigorous continuity-of-slope or continuity-of-wave-function conditions to be applied at the surface S. We have found instead that we can satisfy the boundary conditions that result from requiring Hermiticity of the equation set. We shall exhibit conditions that can be applied to the envelope functions $F_j^\sigma(r)$ to ensure that two solutions are orthogonal to each other and that their energies are real. This orthogonality and reality will guarantee Hermiticity.

We first obtain the coupled differential equations that the envelope functions satisfy in each region separately. By replacing k_μ with $1/i(\partial/\partial x_\mu)$ in the standard derivation of the $\mathbf{k}\cdot\mathbf{p}$ equations, we get

$$\left[-\frac{\hbar^2}{2m}\nabla^2+E_j^\sigma-E\right]F_j^\sigma(r)+\frac{\hbar}{im}\sum_{k=1}^{N}\sum_{\mu}p_{jk}^\sigma(\mu)\frac{\partial}{\partial x_\mu}F_k^\sigma(r)-\frac{\hbar^2}{2m}\sum_{k=1}^{N}\sum_{\mu,\nu}D_{jk}^\sigma(\mu,\nu)\frac{\partial}{\partial x_\mu}\frac{\partial}{\partial x_\nu}F_k^\sigma(r)=0 \ , \tag{2.1}$$

where $\sigma=A$ or B and where

$$D_{jk}^\sigma(\mu,\nu)\equiv 2\sum_{n=N+1}^{\infty}\frac{p_{jn}^\sigma(\mu)p_{nk}^\sigma(\nu)}{m(E_0-E_n^\sigma)} \tag{2.2}$$

and

$$p_{jk}^\sigma(\mu)=\frac{1}{\Omega_c}\int_{\Omega_c}u_j^\sigma(r)^*\frac{\hbar}{i}\frac{\partial}{\partial x_\mu}u_k^\sigma(r)d^3r \ . \tag{2.3}$$

E_0 is some fixed energy near the middle of the energy range of interest.

Notice that

$$\frac{\partial}{\partial x_\mu}\frac{\partial}{\partial x_\nu}=\frac{\partial}{\partial x_\nu}\frac{\partial}{\partial x_\mu} \ .$$

Therefore, any component of $D_{jk}^\sigma(\mu,\nu)$ that is odd under interchange of μ and ν will not contribute to the sum in (2.1) and it is useful to replace $D_{jk}^\sigma(\mu,\nu)$ by its symmetrized form

$$D_{jk}^\sigma(\mu,\nu)\rightarrow\tfrac{1}{2}[D_{jk}^\sigma(\mu,\nu)+D_{jk}^\sigma(\nu,\mu)]$$

$$=\sum_n\frac{p_{jn}^\sigma(\mu)p_{nk}^\sigma(\nu)+p_{jn}^\sigma(\nu)p_{nk}^\sigma(\mu)}{m(E_0-E_n^\sigma)} \ . \tag{2.4}$$

We now apply a standard method for demonstrating orthogonality of two solutions to the equations: Let $F_j^\sigma(z)$ be the solution of (2.1) with energy $E=E_1$. Set

$E=E_1$. Let $G_j^\sigma(z)$ be the solution at $E=E_2$. Multiply (2.1) by $G_j^\sigma(z)^*$, and sum on j. Then repeat the procedure for Eq. (2.1) at $E=E_2$ [so that the envelope functions are $G_k^\sigma(r)$], multiply by $F_j^\sigma(r)^*$, and sum over j. Take the complex conjugate of this latter equation set. Subtract the two equation sets from each other, integrate over regions A and B separately and add the two integrals. The result can be arranged as

$$-\frac{\hbar^2}{2m}\sum_j\int_{A+B}d^3r[G_j^\sigma(r)^*\nabla^2F_j^\sigma(r)-F_j^\sigma(r)\nabla^2G_j^\sigma(r)^*]$$
$$+\frac{\hbar}{im}\sum_{j,k,\mu}\int_{A+B}d^3r\,p_{jk}^\sigma(\mu)\left[G_j^\sigma(r)^*\frac{\partial}{\partial x_\mu}F_k^\sigma(r)+F_k^\sigma(r)\frac{\partial}{\partial x_\mu}G_j^\sigma(r)^*\right]$$
$$-\frac{\hbar^2}{2m}\sum_{j,k,\mu,\nu}\int_{A+B}d^3r\,D_{jk}^\sigma(\mu,\nu)\left[G_j^\sigma(r)^*\frac{\partial}{\partial x_\mu}\frac{\partial}{\partial x_\nu}F_k^\sigma(r)-F_k^\sigma(r)\frac{\partial}{\partial x_\mu}\frac{\partial}{\partial x_\nu}G_j^\sigma(r)^*\right]$$
$$=(E_1-E_2^*)\sum_j\int_{A+B}d^3r\,G_j^\sigma(r)^*F_j^\sigma(r)\,. \tag{2.5}$$

All the terms on the left-hand side (lhs) can be integrated exactly, in the sense that they can be expressed as integrals over the surfaces S and S_0 rather than as volume terms over the regions A and B. For the first-order term, we have

$$\frac{\hbar}{im}\sum_{j,k,\mu}\int_{A+B}p_{jk}^\sigma(\mu)\left[G_j^\sigma(r)^*\frac{\partial}{\partial x_\mu}F_k^\sigma(r)+F_k^\sigma(r)\frac{\partial}{\partial x_\mu}G_j^\sigma(r)^*\right]d^3r=\frac{\hbar}{im}\sum_{\sigma=A,B}\sum_{j,k}\mathbf{p}_{jk}^\sigma\cdot\int_\sigma\nabla G_j^\sigma(r)^*F_k^\sigma(r)d^3r \tag{2.6a}$$
$$=\frac{\hbar}{im}\sum_{\sigma=A,B}\sum_{j,k}\mathbf{p}_{jk}^\sigma\cdot\int_{S_\sigma}G_j(r)^*F_k(r)\hat{\mathbf{n}}\,dS\,. \tag{2.6b}$$

In (2.6a), the volume integral extends over the *interior* of the region σ. In (2.6b), which follows from (2.6a) via use of Gauss's theorem, the surface integral is over the surface S_σ bounding region σ. $\hat{\mathbf{n}}$ is a unit vector, normal to the surface, and directed outward from region σ. Thus, there will be an integral over S_0, the surface bounding region A, and *two* integrals over the surface S, one because S is the inner surface for region A, the other because S is the outer surface for region B.

For the second-order terms, we note that

$$\frac{\partial}{\partial x_\mu}\left[g^*\frac{\partial}{\partial x_\nu}f-f\frac{\partial}{\partial x_\nu}g^*\right]=g^*\frac{\partial}{\partial x_\mu}\frac{\partial}{\partial x_\nu}f-f\frac{\partial}{\partial x_\mu}\frac{\partial}{\partial x_\nu}g^*+\left[\frac{\partial g^*}{\partial x_\mu}\frac{\partial f}{\partial x_\nu}-\frac{\partial f}{\partial x_\mu}\frac{\partial g^*}{\partial x_\nu}\right]. \tag{2.7}$$

The term in large parentheses on the rhs is antisymmetric with respect to the interchange $\mu\leftrightarrow\nu$. Therefore, when we multiply by $D_{jk}^\sigma(\mu,\nu)$ (which is symmetric with respect to the interchange $\mu\leftrightarrow\nu$) this term drops out, leaving

$$\sum_{\mu,\nu}D_{jk}^\sigma(\mu,\nu)\left[g^*\frac{\partial}{\partial x_\mu}\frac{\partial}{\partial x_\nu}f-f\frac{\partial}{\partial x_\mu}\frac{\partial}{\partial x_\nu}g^*\right]$$
$$=\sum_{\mu,\nu}D_{jk}^\sigma(\mu,\nu)\frac{\partial}{\partial x_\mu}\left[g^*\frac{\partial}{\partial x_\nu}f-f\frac{\partial}{\partial x_\nu}g^*\right]. \tag{2.8}$$

On the rhs we can write

$$\sum_\mu D_{jk}^\sigma(\mu,\nu)\frac{\partial}{\partial x_\mu}=\mathbf{D}_{jk}^\sigma(\nu)\cdot\nabla\,, \tag{2.9}$$

where $\mathbf{D}_{jk}^\sigma(\nu)$ is a vector whose μth component is $D_{jk}^\sigma(\mu,\nu)$. Integrating over the interior of region σ, and using Gauss's theorem now gives

$$\sum_{\mu,\nu}D_{jk}^\sigma(\mu,\nu)\int_\sigma d^3r\left[g^*\frac{\partial}{\partial x_\mu}\frac{\partial}{\partial x_\nu}f-f\frac{\partial}{\partial x_\mu}\frac{\partial}{\partial x_\nu}g^*\right]$$
$$=\sum_\nu\mathbf{D}_{jk}^\sigma(\nu)\cdot\int_{S\sigma}\left[g^*\frac{\partial}{\partial x_\nu}f-f\frac{\partial}{\partial x_\nu}g^*\right]\hat{\mathbf{n}}\,dS$$

or, expressing $\mathbf{D}$ and $\hat{\mathbf{n}}$ in terms of components,

$$=\sum_{\mu,\nu}D_{jk}^\sigma(\mu,\nu)\int_{S_\sigma}\left[g^*\frac{\partial}{\partial x_\nu}f-f\frac{\partial}{\partial x_\nu}g^*\right]\hat{\mathbf{n}}_\mu dS\,. \tag{2.10}$$

We have thus converted the lhs of Eq. (2.5) into a sum of surface integrals

$$\sum_{\sigma=A,B}\sum_\mu\int_{S_\sigma}\Omega_\mu^\sigma(r)\hat{\mathbf{n}}_\mu dS\,,$$

where, referring back to (2.5),

$$\Omega_\mu^\sigma(r)\equiv-\frac{\hbar^2}{2m}\sum_j\left[G_j^\sigma(r)^*\frac{\partial}{\partial x_\mu}F_j^\sigma(r)-F_j^\sigma(r)\frac{\partial}{\partial x_\mu}G_j^\sigma(r)^*\right]+\frac{\hbar}{im}\sum_{j,k}p_{jk}^\sigma(\mu)G_j^\sigma(r)^*F_k^\sigma(r)$$
$$-\frac{\hbar^2}{2m}\sum_{j,k,\nu}D_{jk}^\sigma(\mu,\nu)\left[G_j^\sigma(r)^*\frac{\partial}{\partial x_\nu}F_k^\sigma(r)-F_k^\sigma(r)\frac{\partial}{\partial x_\nu}G_j^\sigma(r)^*\right]. \tag{2.11}$$

We define vectors $\mathbf{S}_j^\sigma(r)$ and $\mathbf{T}_j^\sigma(r)$ by

$$\mathbf{S}_j^\sigma(r)\equiv\nabla F_j^\sigma(r)+\frac{i}{\hbar}\sum_k\mathbf{p}_{jk}^\sigma F_k^\sigma(r)+\sum_k\mathbf{D}_{jk}^\sigma\cdot\nabla F_k^\sigma(r)\ , \tag{2.12a}$$

$$\mathbf{T}_j^\sigma(r)\equiv\nabla G_j^\sigma(r)+\frac{i}{\hbar}\sum_k\mathbf{p}_{jk}^\sigma G_k^\sigma(r)+\sum_k\mathbf{D}_{jk}^\sigma\cdot\nabla G_k^\sigma(r)\ . \tag{2.12b}$$

This allows us to write

$$\mathbf{\Omega}^\sigma(r)=-\frac{\hbar^2}{2m}\sum_j[G_j^\sigma(r)^*\mathbf{S}_j^\sigma(r)-F_j^\sigma(r)\mathbf{T}_j^\sigma(r)^*]\ . \tag{2.13}$$

We refer to $\mathbf{S}_j^\sigma(r)$ and $\mathbf{T}_j^\sigma(r)$ as envelope gradients of $F_j^\sigma(r)$ and $G_j^\sigma(r)$, respectively.

Equation (2.5) now becomes

$$(E_1-E_2^*)\sum_j\int_{A+B}d^3r\,G_j^\sigma(r)^*F_j^\sigma(r)=\sum_\sigma\int_{S_\sigma}\Omega^\sigma(r)\cdot\hat{\mathbf{n}}\,dS \tag{2.14}$$

and the condition that the solutions be orthogonal is

$$\sum_\sigma\int_{S_\sigma}\mathbf{\Omega}^\sigma(r)\cdot\hat{\mathbf{n}}\,dS=0\ . \tag{2.15}$$

This gives rise to two conditions. The first is that the integral over the outer surface S_0 vanishes,

$$\int_{S_0}\mathbf{\Omega}^A(r_0)\cdot\hat{\mathbf{n}}\,dS_0=0\ . \tag{2.16}$$

The second is that the normal component of Ω is continuous across the inner interface, i.e., that for r on the surface S,

$$[\mathbf{\Omega}^A(r)-\mathbf{\Omega}^B(r)]\cdot\hat{\mathbf{n}}=0\ . \tag{2.17}$$

A number of familiar boundary conditions satisfy (2.16). If the solutions all vanish on the outer surface, i.e., if

$$F_j^n(r_0)=0,\quad r_0\text{ on }S_0\ , \tag{2.18}$$

or if the surface is one for which periodic boundary conditions can be applied, or if solutions vanish over part of S_0 and are periodic over other parts, then (2.16) will be satisfied. In order to satisfy (2.17), we can make each envelope function $F_j^\sigma(r)$ and each normal component of the envelope gradient continuous across the surface S

$$F_j^A(r)=F_j^B(r),\quad r\text{ on }S\ , \tag{2.19a}$$

$$S_j^A(r)\cdot\hat{\mathbf{n}}=\mathbf{S}_j^B(r)\cdot\hat{\mathbf{n}},\quad r\text{ on }S\ . \tag{2.19b}$$

These boundary continuity conditions must hold for solutions at any energy. Therefore, the solution at E_2 must also satisfy the same condition, namely,

$$G_j^A(r)=G_j^B(r),\quad\text{on }S\ , \tag{2.19c}$$

$$\mathbf{T}_j^A(r)\cdot\hat{\mathbf{n}}=\mathbf{T}_j^B(r)\cdot\hat{\mathbf{n}}\ . \tag{2.19d}$$

If (2.19) is satisfied, then (2.17) will be true.

In order to demonstrate that the energy E_1 is real, one can repeat the derivation just given with E_1, $F_j^\sigma(r)$, and $\mathbf{S}_j^\sigma(r)$ replacing E_2, $G_j^\sigma(r)$, and $\mathbf{T}_j^\sigma(r)$, respectively. Equation (2.14) then can be solved for $\mathrm{Im}E_1$, which can be shown to vanish if (2.15) holds true. A somewhat tedious evaluation of the current $\mathbf{J}(r)$ averaged over a unit cell in region σ, and dropping higher-order terms, gives

$$\bar{J}^\sigma=\frac{\hbar}{m}\mathrm{Im}\sum_j F_j^\sigma(r)^*\mathbf{S}_j^\sigma(r) \tag{2.20}$$

which means that (2.19) also gives continuity of the normal component of the (cell-averaged) current at the internal interface.

On comparing (2.20) with the formal expression for the current in terms of the full wave function

$$J(r)=\frac{\hbar}{m}\mathrm{Im}[\psi(r)^*\nabla\psi(r)]\ ,$$

one notes that if $F_j^\sigma(r)$ plays the role of the wave function in envelope-function space then $\mathbf{S}_j^\sigma(r)$, its envelope gradient, plays the role of the spatial gradient in this same envelope-function space.

III. DERIVATION OF THE EXPRESSIONS FOR THE MATRIX ELEMENTS

We now specialize to the quantum-wire geometry used by Gershoni *et al.*[1] The system is uniform in the z direction, but its properties in the x,y plane are piecewise constant. Boundaries between different regions in the plane are straight lines parallel to either the x or to the y axis, as shown in Fig. 2. A particular region σ covers the interior of the region defined by

$$x_{m-1}<x<x_m\ ,\quad m=1,2,\ldots,M_X\ , \tag{3.1a}$$

$$y_{n-1}<y<y_n,\quad n=1,2,\ldots,N_Y\ . \tag{3.1b}$$

Within each region σ, the envelope functions $F_j^\sigma(r)$

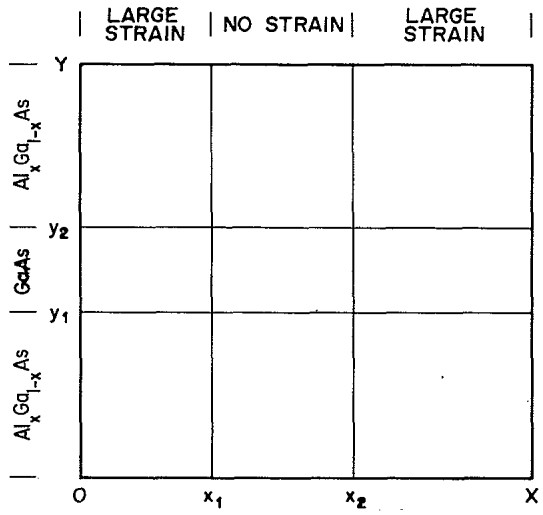

FIG. 2. Geometry used in the quantum-wire problem. The system is uniform in the z direction but composed of rectangular regions where the materials properties are independent of position within a region but may change discontinuously between regions.

satisfy the following set of coupled differential equations:

$$\sum_k \left[-\frac{\hbar^2}{2m_0} \sum_{\mu,\nu} D^\sigma_{jk}(\mu,\nu) \frac{\partial}{\partial x_\mu} \frac{\partial}{\partial x_\nu} + \frac{\hbar}{i} \sum_\mu p^\sigma_{jk}(\mu) \frac{\partial}{\partial x_\mu} + V^\sigma_{jk} - E\delta_{jk} \right] F^\sigma_k(r) = 0 \ . \quad (3.2)$$

The second-order constants D^σ_{jk} now contain a $\delta_{jk}\delta_{\mu\nu}$ contribution [which gives rise to the $-(\hbar^2/2m_0)\nabla^2\delta_{jk}$ term of Eq. (2.1)], plus terms like (2.4), the Kane parameters for the material.[25,26] The matrix $D^\sigma_{jk}(\mu,\nu)$ is real and dimensionless. In addition, it is symmetric with respect to index interchanges $j \leftrightarrow k$ and $\mu \leftrightarrow \nu$ separately.

When dealing with systems for which spin-orbit coupling in the valence band is important, one has a choice of whether to use $|x\uparrow\rangle, |y\uparrow\rangle, \ldots, |z\downarrow\rangle$ zone-center Bloch waves, or instead to use the linear combinations which diagonalize the spin-orbit interaction at Γ. In the present problem, there is no advantage in first diagonalizing the spin-orbit interaction, and it will be simplest to use the $|x\uparrow\rangle, \ldots |z\downarrow\rangle$ basis.

The matrices $p^\sigma_{jk}(\mu)$ are momentum matrix elements. They are pure imaginary and Hermitian.[26] We neglect strain for now. The matrix V^σ_{jk} then consists of two terms,

$$V^\sigma_{jk} = E^\sigma_j \delta_{jk} + \Delta^\sigma_{jk} \ . \quad (3.3)$$

E^σ_j is the band-edge energy and Δ^σ_{jk} is the k-independent part of the spin-orbit coupling.

Equation (3.2) has to be supplemented by outer boundary conditions plus internal interface-matching conditions. For the outer boundary conditions, we take the envelope functions to be periodic on the four outer boundary planes parallel to the z axis, with the intention of locating these planes far enough out that two-dimensional confinement of the wave function will prevent it from reaching them. Alternatively, these equations describe the k_Γ state of superlattices in one or two dimensions if the wave functions do reach the outer boundaries. (There is a simple way to study the superlattice dispersion, but we shall defer that until Sec. V.) The periodicity condition forces us to equate material constants in the regions adjacent to the outer boundary so that there is no discontinuity across them. We also impose periodic boundary conditions at 0 and Z, where Z is aribtrary. These boundary conditions ensure that (2.16) is satisfied.

For the internal interface conditions, we take (2.19a) and (2.19b). Because the free-electron kinetic energy is now incorporated into D^σ_{jk}, the definition (2.12a) is now altered to

$$\mathbf{S}^\sigma_j(r) \equiv \frac{i}{\hbar} \sum_k \mathbf{p}^\sigma_{jk} F^\sigma_k(r) + \sum_k \mathbf{D}^\sigma_{jk} \cdot \nabla F^\sigma_k(r) \ . \quad (3.4)$$

The system is finite in all three directions. It extends over $0 \le x < X$, $0 \le y < Y$, and $0 < z < Z$. Let

$$\phi_m(x) = \sqrt{1/X}\, e^{2\pi i m x/X} \ , \quad (3.5a)$$

$$\psi_n(y) = \sqrt{1/Y}\, e^{2\pi i n y/Y} \ , \quad (3.5b)$$

$$\varepsilon_p(z) = \sqrt{1/Z}\, e^{2\pi i p z/Z} \ . \quad (3.5c)$$

These functions are mutually orthonormal and they satisfy the outer boundary condition (2.16). We expand the envelope function as

$$F^\sigma_j(r) = \sum_m^\infty \sum_n^\infty \sum_p^\infty F_j(m,n,p) \phi_m(x) \psi_n(y) \varepsilon_p(z)$$

$$\equiv \sum_\alpha F_j(\alpha) \theta_\alpha(r) \ , \quad (3.6b)$$

where

$$\theta_\alpha(r) \equiv \phi_m(x) \psi_n(y) \varepsilon_p(z) \ , \quad (3.6c)$$

$$\alpha \equiv (m,n,p) \ . \quad (3.6d)$$

Notice that there is no region index σ on $F_j(\alpha)$: We use the *same* expansion coefficients in every region σ. This will automatically satisfy the envelope-function continuity condition (2.19a) because the expansion functions $\theta_\alpha(r)$ are themselves continuous. It fails to satisfy the slope discontinuity condition (2.19b) at the interface because the functions $\theta_\alpha(r)$ have gradients that are continuous. This causes no problem, because it is well known[27] how expansions of the general form (3.4) converge in the case of functions having a finite number of finite discontinuities or, as is the case here, continuous functions having a finite number of slope discontinuities. The only caution we must observe is not to differentiate the series, because each derivative worsens or destroys its convergence.[27] Accordingly, we may obtain equations governing the $F_j(\alpha)$ by multiplying (3.2) by $\theta_\alpha(r)^*$, integrating over each region σ, and then, before summing over all regions σ, applying Gauss's theorem or Green's theorem so that the derivatives all work on $\theta_\alpha(r)^*$, not on $F^\sigma_j(r)$. *It is this step that introduces specifically interface terms into the matrix elements.*

For the first step, integration over a single region σ, we obtain

$$\sum \int_\sigma d^3r\, \theta_\alpha(r)^* \left[-\frac{\hbar^2}{2m_0} \sum_{\mu,\nu} D^\sigma_{jk}(\mu,\nu) \frac{\partial}{\partial x_\mu} \frac{\partial}{\partial x_\nu} + \frac{\hbar}{i} \sum_\mu p^\sigma_{jk}(\mu) \frac{\partial}{\partial x_\mu} + V^\sigma_{jk} - E\delta_{jk} \right] F^\sigma_k(r)$$
$$= \sum \int_\sigma d^3r\, F^\sigma_k(r) \left[-\frac{\hbar^2}{2m_0} \sum_{\mu,\nu} D^\sigma_{jk}(\mu,\nu) \frac{\partial}{\partial x_\mu} \frac{\partial}{\partial x_\nu} - \frac{h}{i} \sum_\mu p^\sigma_{jk}(\mu) \frac{\partial}{\partial x_\mu} + V^\sigma_{jk} - E\delta_{jk} \right] \theta_\alpha(r)^*$$
$$+ \sum_\mu \int_{S_\sigma} \Omega^{\sigma\alpha}_{j\mu}(r_s) \hat{\mathbf{n}}_\mu dS = 0 \ . \tag{3.7}$$

Here, S_σ is the surface surrounding the region σ, r_s is a position on the surface, and $\hat{\mathbf{n}}$ is the outer directed normal to the surface. The integrand is defined as

$$\Omega^{\sigma\alpha}_{j\mu}(r) \equiv \frac{\hbar^2}{2m_0} \sum_{\nu,k} D^\sigma_{jk}(\mu,\nu) \left[\theta_\alpha(r)^* \frac{\partial}{\partial x_\nu} F^\sigma_k(r) - F^\sigma_k(r) \frac{\partial}{\partial x_\nu} \theta^*_\alpha(r) \right] + \frac{\hbar}{im_0} \sum_k \theta_\alpha(r)^* p^\sigma_{jk}(\mu) F^\sigma_k(r) \ . \tag{3.8}$$

A part of (3.8) will be continuous across the interface and a part will be discontinuous. The normal component of the vector $\mathbf{S}^\sigma_j(r)$ given by Eq. (3.4) and $F^\sigma_k(r)$ are continuous. For that reason, we rewrite (3.8) as

$$\mathbf{\Omega}^{\sigma\alpha}_j(r) = -\frac{\hbar^2}{2m_0} \theta_\alpha(r)^* \mathbf{S}^\sigma_j(r) + \sum_k F_k(r) \mathbf{U}^{\sigma\alpha}_{jk}(r) \ , \tag{3.9}$$

where

$$\mathbf{U}^{\sigma\alpha}_{jk} = \frac{\hbar^2}{2m_0} \mathbf{D}^\sigma_{jk} \cdot \nabla \theta_\alpha(r)^* + \frac{\hbar}{2im_0} \mathbf{p}^\sigma_{jk} \theta_\alpha(r)^* \ . \tag{3.10}$$

We now sum (3.6) over all regions σ. The sum over all the surface terms is

$$S^\alpha_j = \sum_\sigma \int_{S_\sigma} \hat{\mathbf{n}}\, dS \cdot \left[-\frac{\hbar^2}{2m_0} \theta^*_\alpha(r_s) \mathbf{S}^\sigma_j(r_s) + \sum_k \mathbf{U}^{\sigma\alpha}_{jk}(r_s) F_k(r_s) \right] . \tag{3.11}$$

There is no contribution to S^α_j from the outer boundary planes because $\theta_\alpha(r)^*$ and $F_k(r)$ are periodic. Each internal plane is integrated over twice, once as a boundary of the region σ' on its left, and again as boundary of the region σ on its right. Because of the reversal of $\hat{\mathbf{n}}$ on these two integrations, one is left with integrating the discontinuity of $\hat{\mathbf{n}} \cdot \mathbf{\Omega}^{\sigma\alpha}_j$ over the boundary. The functions θ^*_α are continuous. The functions F^σ_j and $\hat{\mathbf{n}} \cdot \mathbf{S}^\sigma_j$ are continuous because of our interface conditions (2.19). Thus (3.11) picks up only the contribution from the interface discontinuity of $\hat{\mathbf{n}} \cdot \mathbf{U}^\sigma_{jk}$.

We now evaluate. Let $S_{\sigma'\sigma}$ be the particular interface plane separating two *adjacent* regions σ' and σ. Let $\hat{\mathbf{n}}$ be normal to that interface, pointing from σ' to σ. Then (3.11) equals the following sum over internal interfaces only:

$$S^\alpha_j = \frac{\hbar^2}{2m_0} \sum_{\sigma',\sigma} \sum_k \sum_{\mu,\nu} \int_{S\sigma',\sigma} dS\, F_k(r_s) \hat{\mathbf{n}}_\mu [D^{\sigma'}_{jk}(\mu,\nu) - D^\sigma_{jk}(\mu,\nu)] \frac{\partial}{\partial x_\nu} \theta_\alpha(r_s)^*$$
$$+ \frac{\hbar}{2im_0} \sum_{\sigma',\sigma} \sum_k \sum_\mu \int_{S_{\sigma'\sigma}} dS\, F_k(r_s) \hat{\mathbf{n}}_\mu [p^{\sigma'}_{jk}(\mu) - p^\sigma_{jk}(\mu)] \theta_\alpha(r_s)^* \ . \tag{3.12}$$

Because of the symmetry $D(\mu,\nu) = D(\nu,\mu)$, the antisymmetric part of $\hat{\mathbf{n}}_\mu \partial x_\nu$ will not contribute, and so we make the replacement

$$\hat{\mathbf{n}}_\mu \frac{\partial}{\partial x_\nu} \to \frac{1}{2} \left[\hat{\mathbf{n}}_\mu \frac{\partial}{\partial x_\nu} + \hat{\mathbf{n}}_\nu \frac{\partial}{\partial x_\mu} \right] \tag{3.13}$$

in (3.12). At this point, we can now insert

$$F_k(r) = \sum_{m'} \sum_{n'} \sum_{p'} F_k(m',n',p') \phi_{m'}(x) \psi_{n'}(y) \varepsilon_{p'}(z) \tag{3.14}$$

and we use

$$\frac{\partial}{\partial z} \theta_\alpha(r_s)^* = -iK_p \theta_\alpha(r_s)^* \ , \tag{3.15a}$$

$$K_p = 2\pi p / Z \ . \tag{3.15b}$$

The z integral gives $\delta_{pp'}$. What remains is

$$S^j_\alpha = \sum_k \sum_{m',n'} S_{jk}(m,n;m',n',K_p) F_k(m',n',p) \ , \tag{3.16a}$$

where

$$S_{jk}(m,n;m',n',K_p)\equiv\frac{\hbar^2}{2m_0}\sum_{\sigma',\sigma}\sum_{\mu,\nu}\int_{S_{\sigma'\sigma}}dS\,\phi_{m'}\psi_{n'(y)}[D^{\sigma'}_{jk}(\mu,\nu)-D^{\sigma}_{jk}(\mu,\nu)]\frac{1}{2}\left[\hat{\mathbf{n}}_\mu\frac{\partial}{\partial x_\nu}-\hat{\mathbf{n}}_\nu\frac{\partial}{\partial x_\mu}\right]\phi_m(x)^*\psi_n(y)^*$$
$$+\frac{\hbar}{2im_0}\sum_{\sigma',\sigma}\sum_{\mu}\int_{S_{\sigma'\sigma}}dS\,\phi_{m'}(x)\psi_{n'}(y)[p^{\sigma'}_{jk}(\mu)-p^{\sigma}_{jk}(\mu)]\hat{\mathbf{n}}_\mu\phi_m(x)^*\psi_n(y)^*\ . \tag{3.16b}$$

Next, we consider the volume integrals appearing in (3.7). We substitute (3.14) and get

$$\sum_{\sigma}\sum_{k}\sum_{m'}\sum_{n'}\sum_{p'}F_k(m',n',p')\int_\sigma d^3r\,\phi_{m'}(x)\psi_{n'}(y)\varepsilon_{p'}(z)$$
$$\times\left[-\frac{\hbar^2}{2m_0}\sum_{\mu,\nu}D^{\sigma}_{jk}(\mu,\nu)\frac{\partial}{\partial x_\mu}\frac{\partial}{\partial x_\nu}-\frac{\hbar}{im_0}\sum_{\mu}p^{\sigma}_{jk}(\mu)\frac{\partial}{\partial x_\mu}+V^{\sigma}_{jk}\right]\phi^*_m(x)\psi^*_n(y)\varepsilon^*_p(z)$$
$$=\sum_{\sigma}\sum_{k}\sum_{m'}\sum_{n'}B^{\sigma}_{jk}(m,n;m',n',K_p)F_k(m',n',p)\ , \tag{3.17}$$

where

$$B^{\sigma}_{jk}(m,n;m',n',K_p)=\int_\sigma dx\,dy\,\phi'_m(x)\psi_{n'}(y)\left[-\frac{\hbar^2}{2m_0}\sum_{\mu,\nu}D^{\sigma}_{jk}(\mu,\nu)\frac{\partial}{\partial x_\mu}\frac{\partial}{\partial x_\nu}-\frac{\hbar}{im_0}\sum_{\mu}p^{\sigma}_{jk}(\mu)\frac{\partial}{\partial x_\mu}+V^{\sigma}_{jk}\right]\phi^*_m(x)\psi^*_n(y)\ , \tag{3.18a}$$

and where

$$\frac{\partial}{\partial z}\equiv -iK_p\ . \tag{3.18b}$$

Finally for the term in (3.6) that is proportional to E, we get

$$\sum_{k}\sum_{m'}\sum_{n'}\sum_{p'}F_k(m',n',p')E\delta_{jk}\sum_{\sigma}\int_\sigma d^3r\phi_{m'}(x)\psi_{n'}(y)\varepsilon_{p'}(z)\phi_m(x)\psi_n(y)\varepsilon_p(z)^*=EF_j(m,n,p)\ . \tag{3.19}$$

because the integral now extends over the volume on which the functions are orthogonal. By this means, we have obtained a matrix eigenvalue equation of the form

$$\sum_{k}\sum_{m'}\sum_{n'}H_{jk}(m,n;m',n',K_p)F_k(m',n',p)$$
$$=E(K_p)F_j(m,n,p)\ , \tag{3.20}$$

where

$$H_{jk}(m,n;m',n',K_p)=\sum_{\sigma}B^{\sigma}_{jk}(m,n;m',n',K_p)$$
$$+S_{jk}(m,n;m',n',K_p)\ . \tag{3.21}$$

The sum of the bulk terms B^σ is over all regions σ. The interface term S_{jk}, which arose because of discontinuities in slope of the envelope functions, is a sum over all internal interfaces.

IV. AN ALTERNATIVE DERIVATION

We have just given a road map of what has to be done to calculate the matrix elements $H_{jk}(m,n;m',n',K_p)$ and an explanation of why it has to be done that way. The derivation, burdened with multiple subscripts and summations, is difficult to follow. In this section, we present a derivation that is simpler and more intuitive. It will involve operations that are heuristic and, apparently, without sufficiently strong justification. First, we will treat the materials parameters p_{jk} and D_{jk} as though they were smooth differentiable functions of position, and then we will place them in front of, behind, or between partial differential operators in a way that is seemingly arbitrary. The placements we will choose do make the Hamiltonian Hermitian, but there are several different placements we could have chosen to produce a Hermitian Hamiltonian. Second, we will let the r dependence in the material parameters be such that they become piecewise constant:

$$p_{jk}(r)\rightarrow p^{\sigma}_{jk}\ ,\quad r\text{ in }\sigma \tag{4.1a}$$

$$D_{jk}(r)\rightarrow D^{\sigma}_{jk},\quad r\text{ in }\sigma\ . \tag{4.1b}$$

The (infinitely) rapid change at the boundaries of each region σ is not compatible with the assumption (slowly changing parameters) on which the envelope-function approximation is based. Third, we will expand the envelope functions in the Fourier series (3.5) and (3.6) and differentiate that series, knowing that the resulting first derivatives converge to the wrong value at the interfaces and that the second derivatives do not converge there at all. The equations derived in this way cannot be valid at the internal interfaces, yet we are going to integrate these equations across the interfaces and obtain interface-matching conditions thereby.

The justification for all of this lies in the first step, our choice of how the materials parameters are placed rela-

tive to the partial differential operators. We make this choice in such a way that, when the succeeding (unjustified) operations are carried out, the result will be equivalent to what we have already obtained using the correct (but complicated) derivation presented in Secs. II and III. By this means we offer a prescription for constructing the matrix elements H_{jk} that is both easy to follow and (from the point of view of the result) is correct.

Specifically, let us consider an eight-band model, in which the basis states (the zone-center Bloch waves) are $|s\uparrow\rangle$, $|x\uparrow\rangle$, $|y\uparrow\rangle$, $|z\uparrow\rangle$ and their time reversed conjugates, $|s\downarrow\rangle$, $|x\downarrow\rangle$, $|y\downarrow\rangle$, $|z\downarrow\rangle$. This basis set is said to be a Kramers basis (an even number of basis functions with each function in the second half of the basis being the time-reverse conjugate of the corresponding function in the first half.) In such a basis, the matrix of any time-reversal-invariant operator H can be written as

$$\mathbf{H}=\begin{bmatrix} \mathbf{G} & \mathbf{\Gamma} \\ -\mathbf{\Gamma}^* & G^* \end{bmatrix} \tag{4.2a}$$

or, if the matrix is k dependent, as

$$\mathbf{H}(\mathbf{k})=\begin{bmatrix} \mathbf{G}(\mathbf{k}) & \mathbf{\Gamma}(\mathbf{k}) \\ -\mathbf{\Gamma}^*(-\mathbf{k}) & \mathbf{G}^*(-\mathbf{k}) \end{bmatrix}, \tag{4.2b}$$

where G and T are both square matrices. (In the actual matrix we will use, Γ will turn out to be independent of $\mathbf{k}$.) The $\mathbf{k}\cdot\mathbf{p}$ Hamiltonian used in the usual envelope-function-equation set is time-reversal invariant. Its elements therefore have the form (4.2). The matrix $\mathbf{G}$ can be written as

$$\mathbf{G}=\mathbf{G}_1+\mathbf{G}_2+\mathbf{G}_{\rm so}\ , \tag{4.3a}$$

where

$$\mathbf{G}_1\equiv\begin{bmatrix} E_c & iPk_x & iPk_y & iPk_z \\ -iPk_x & E_v & 0 & 0 \\ -iPk_y & 0 & E_v & 0 \\ -iPk_z & 0 & 0 & E_v \end{bmatrix}, \tag{4.3b}$$

$$\mathbf{G}_2\equiv\begin{bmatrix} A'k^2 & Bk_yk_z & Bk_xk_z & Bk_xk_y \\ Bk_yk_z & L'k_x^2+M(k_y^2+k_z^2) & Nk_xk_y & Nk_xk_z \\ Bk_zk_x & Nk_xk_y & L'k_y^2+M(k_x^2+k_z^2) & Nk_yk_z \\ Bk_xk_y & Nk_xk_z & Nk_yk_z & L'k_z^2+M(k_x^2+k_y^{2)} \end{bmatrix}, \tag{4.3c}$$

and

$$\mathbf{G}_{\rm so}=-\frac{\Delta}{3}\begin{bmatrix} 0 & 0 & 0 & 0 \\ 0 & 0 & i & 0 \\ 0 & -i & 0 & 0 \\ 0 & 0 & 0 & 0 \end{bmatrix}. \tag{4.3d}$$

The matrix $\mathbf{\Gamma}$ is

$$\mathbf{\Gamma}=-\frac{\Delta}{3}\begin{bmatrix} 0 & 0 & 0 & 0 \\ 0 & 0 & 0 & -1 \\ 0 & 0 & 0 & i \\ 0 & 1 & -i & 0 \end{bmatrix}. \tag{4.3e}$$

The parameters P, A', B, L', M, and N are real numbers, and are defined in Kane's article.[26] Δ is the spin-orbit-splitting parameter and E_c and E_v are the band-edge energies in the absence of spin-orbit coupling.

The operator (4.2) is converted into a differential operator via the replacement

$$ik_\mu\rightarrow\partial/\partial x_\mu \tag{4.4a}$$

and all of the parameters are considered as functions of position. The partials and parameters are then symmetrized according to the scheme

$$P\frac{\partial}{\partial x_\mu}\rightarrow\frac{1}{2}\left[P\frac{\partial}{\partial x_\mu}+\frac{\partial}{\partial x_\mu}P\right], \tag{4.4b}$$

$$Q\frac{\partial}{\partial x_\mu}\frac{\partial}{\partial x_\nu}\rightarrow\frac{1}{2}\left[\frac{\partial}{\partial x_\mu}Q\frac{\partial}{\partial x_\nu}+\frac{\partial}{\partial x_\nu}Q\frac{\partial}{\partial x_\mu}\right], \tag{4.4c}$$

where

$$Q=A',\ B,\ L',\ M,\ \text{and}\ N\ . \tag{4.4d}$$

The 8×8 matrix obtained in this way has elements that we denote as $H_{jk}(r,\nabla)$ and the Schrödinger equation to be solved is

$$\sum_{k=1}^{8}H_{jk}(r,\nabla)F_k(r)=EF_j(r)\ . \tag{4.5}$$

We insert the expansion (3.14) and (3.15) here, multiply by $\phi_m^*(x)\psi_n^*(y)\varepsilon_p^*(z)$ and integrate over the orthogonality region implied by (3.5). The result is equations of the form (3.20) and (3.21). This time, however, the surface terms arise as integrals over the δ functions that appear when the discontinuous parameters $A',\ldots,N$ are differentiated. All of the matrix elements can be evaluated analytically. In the problem formulated in this manner, there is no need for any numerical integrations.

There are two useful checks on the numerical work in

setting up the matrix H. The first is that the matrix H ix Hermitian:

$$H_{jk}(m,n;m',n',K_p)=H_{kj}(m',n';m,n,K_p)^* \ . \quad (4.6)$$

The second is that the matrix, expressed in a Kramers basis, has the form appropriate to a time-reversal-invariant operator. That is, in analogy with (4.2), we will now have

$$H(K_p)=\begin{bmatrix} G(K_p) & \Gamma \\ -\Gamma^* & G^*(-K_p) \end{bmatrix} . \quad (4.7)$$

In (4.7), we have written the matrices as though j, m, and n were the first index and k, m', and n' were the second. In constructing the Kramers basis, we use the fact that $|s\downarrow\rangle$, $|x\downarrow\rangle$, $|y\downarrow\rangle$, and $|z\downarrow\rangle$ are the time-reverse conjugates of $|s\uparrow\rangle$, $|x\uparrow\rangle$, $|y\uparrow\rangle$, and $|z\uparrow\rangle$, while $\phi_{-m}(x)\psi_{-n}(y)$ is the time-reverse conjugate of $\phi_m(x)\psi_n(y)$.

The prescription, as we have described it, assumes that the x,y,z coordinates for describing the geometry of the quantum wire refer to axes that coincide with the crystallographic axes of the underlying crystal. If one finds it convenient to have the quantum-wire geometry defined with respect to other axes x', y', and z', the functions used to expand the envelope will be $\phi_m(x')\phi_n(y')\varepsilon_p(z')$. The easiest procedure to derive the needed equations is to introduce the corresponding wave-space-propagation constants by

$$k'_\mu \rightarrow \frac{1}{i}\frac{\partial}{\partial x'_\mu} ,$$

specify the rotation that expresses k in terms of k'

$$k_\mu=\sum_\nu a_{\mu\nu}k'_\nu , \quad (4.8)$$

and then substitute (4.8) into (4.3b) and (4.3c). At this point, one can drop the primes from both k'_μ and x'_μ and simply repeat all of the steps following Eq. (4.3).

The derivation to this point has neglected strain. In those regions σ where strain is present, the 8×8 Hamiltonian described by Eqs. (4.2) and (4.3) acquires extra terms proportional to strain. The extra terms can be obtained by repeating the original derivation given by Pikus and Bir[28] using Kane's formalism.[26] This has been recently done by Bahder.[29] His results are in exactly the right form to be incorporated into (4.2) and (4.3). In particular, note that Bahder calls attention to the fact that $\mathbf{P}\rightarrow\mathbf{P}(\hat{1}+\hat{\varepsilon})$ when strain in present, something clearly indicated in the Pikus and Bir derivation but apparently ignored by subsequent workers, probably because $\hat{\varepsilon}\ll\hat{1}$ in any practical situation. Optical transitions in a quantum wire produced in part by strain confinement have recently been studied by Gershoni *et al.*[30]

V. SUMMARY AND DISCUSSION

We have shown how to set up the matrix whose eigenfunctions and eigenvalues give the electronic spectrum and multiband envelope functions in a system whose structure corresponds to a "checkerboard" geometry in one, two, or three dimensions. That is, the materials' parameters are constants in regions bounded by planes, but they may vary discontinuously from one region to the next. The technique we used was to expand each envelope function in plane waves and to insert that expansion into the multiband-envelope-function equations. Two derivations for the resulting matrix elements were given. The first was rigorous mathematically. It was based on the condition that the set of equations for the wave functions in several regions had to have an overall Hermitian structure. This imposed boundary matching conditions which were identical to those obtained via the more usual approach of demanding continuity of the normal component of the (unit-cell-averaged) current. The second derivation was much more heuristic. It made use of several seemingly arbitrary steps whose ultimate justification was that they gave a final result identical to that obtained rigorously.

Although the method has been set up to deal with a checkerboard geometry, one can approximate many arbitrary situations within a checkerboard framework, as Fig. 3 shows. Computationally, the time required to calculate the individual Hamiltonian matrix elements will be somewhat increased, but the number of plane waves to achieve convergence will not be affected. It is this latter number that governs the time needed to solve the eigenvalue problem. Because the time required to set up the matrix elements is small compared to that needed for diagonalizing the matrix, the solution for more complicated geometries can be obtained without excessive difficulty.

In order to test the method, we have used it to calculate the spectra, wave functions, and optical absorption for a system with one-dimensional confinement, namely the quantum well studied by Eppenga, Schuurmans, and Colak.[15] In these calculations, the structure is infinite and uniform in two dimensions. Using the parameters given in that paper, we obtain dispersion curves (energy eigenvalues versus $k_\parallel$ along the superlattice axis) and optical matrix elements identical to theirs. [There is, however, an exact factor of 2 discrepancy between their Fig. 2(c) for light polarized in the z direction and our result.

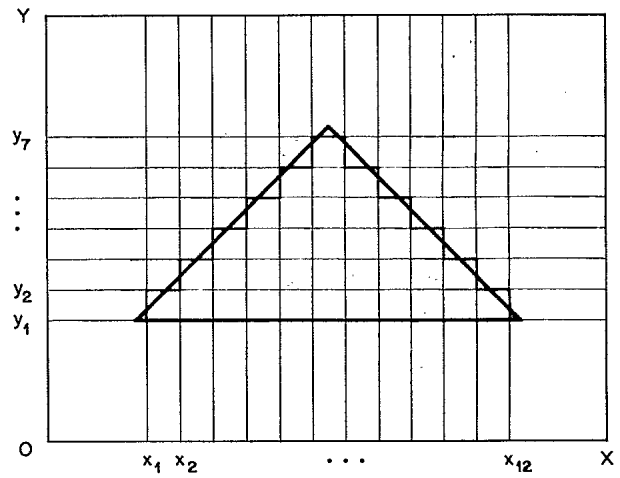

FIG. 3. Use of the checkerboard geometry to approximate a quantum wire of irregular cross section.

This is due to a numerical error on their part, as a comparison of their oscillator strengths at $k_{\|}=0$ shows.] Convergence required our using nine plane waves in the Fourier expansion.

We have also reproduced some of the results of the quantum-wire calculations of Citrin and Chang.[2] Figure 4(a) shows the valence-band states we calculated for a square quantum wire, having a 100×100 Å core of GaAs. This wire is surrounded by barriers of $Al_{0.2}Ga_{0.8}As$. In our calculation, the wires are part of a superlattice array with a 200×200 Å^2 unit cell, so that the barriers between wires are 100 Å thick. This is effectively infinite with regard to the valence-band spectrum, as our calculations with unit cells both of smaller and of larger size have demonstrated. These calculations required 11×11 plane waves for convergence, which we verified by going to 13×13 plane waves for the figures exhibited here. The parameters used in the wire were the same as the GaAs parameters used by Citrin and Chang. The parameters used in the barrier were a weighted average of the GaAs parameters and of the parameters for AlAs, as given by Landolt-Börnstein.[31] In carrying out these calculations, we confirmed Citrin and Chang's guess that the spectrum of valence-band states is not appreciably affected by using parameters for pure GaAs in the barrier, by carrying out complete and converged calculations for both sets of barrier parameters.

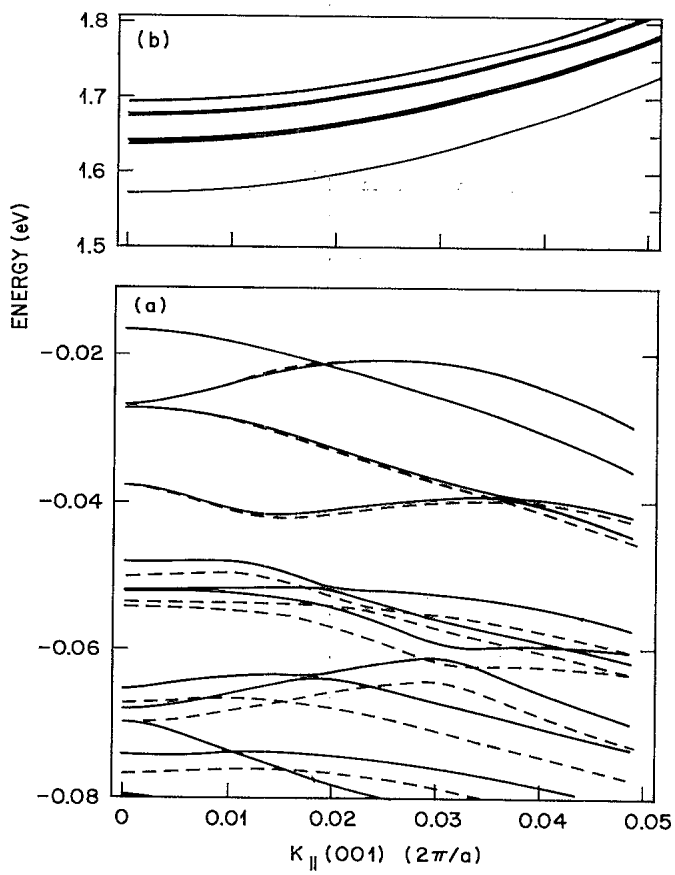

FIG. 4. (a) Energies of the valence-band states vs $k_{\|}$ in a 100×100 Å^2 GaAs wire surrounded by $Al_{0.2}Ga_{0.8}As$ to make a superlattice 200 Å on a side. There is no broadening in these valence-band states due to overlap of the wave functions in adjacent wires or any other superlattice effect. (b) Same as (a) but for the electron states in the same quantum-wire structure. There is now a band of energies at each $k_{\|}$ caused by overlap of the wave functions. The allowed band regions are shaded.

In Fig. 4(a) the results of our calculations are shown as solid lines and those of Fig. 1, Chang and Citrin (CC), are shown by dashed lines. The deviations between the two sets of curves are exactly what is to be expected from CC's discussion of the lack of convergence of their calculation. Their Fig. 1 was produced using an array of 7×7 Gaussian basis functions. They mention that they obtained convergence of the zone-center spectra by using 11×11 Gaussians and that the converged spectra were higher than those exhibited by amounts that ranged from 0.4% for the highest band to 3% for the lowest. That deviation is exactly what we have found here. The two uppermost valence bands are so similar in both calculations that the dashed lines are not readily apparent.

The CC calculation was carried out for a true quantum-wire geometry, using localized basis functions to represent the envelope functions. Our calculation used a discrete Fourier expansion to represent the envelope functions; and so it introduced, in effect, a superlattice of quantum wires. The effect of the superlattice band structure is easily accommodated into the calculational scheme by replacing [see Eq. (3.5)].

$$2\pi m/X \rightarrow 2\pi m/X + q_x \ , \tag{5.1a}$$

$$2\pi n/Y \rightarrow 2\pi n/Y + q_y \ , \tag{5.1b}$$

where q_x and q_y are confined to the first Brillouin zone of the superlattice. Having calculated the spectrum both at the superlattice zone center and at the zone corner, we found no broadening of the valence-band states due to superlattice effects, e.g., overlap of the wave function in one unit cell with that in the next. This is exactly what one would expect for a unit cell which had been made large enough to make the zone-center spectra independent of cell size.

The conduction-band states *are* affected by the choice of parameters for the barrier material. The increased sensitivity of the electron states to the barrier parameters comes about because these states penetrate further into the barrier. That penetration is large enough that the 200×200 Å^2 unit cell is too small to isolate the wires from each other. Superlattice effects set in. Instead of a discrete spectrum for each k_z, there is a band of states at each k_z, with an individual state in each band being characterized by q_x and q_y, propagation constants for the superlattice band structure.

Our spectrum of conduction-band states, calculated using barrier parameters for $Al_{0.2}Ga_{0.8}As$, is shown in Fig. 4(b). This figure is a composite of two calculations, one with $q_x=q_y=0$, the other with $q_x=\pi/X$, $q_y=\pi/Y$. These two will produce the lower and upper limits of the superlattice bands. The difference between them, the band width, is negligible for the lowest electron band and is more apparent for the next two bands. In the limit of a

very large unit cell, the upper and lower edges should converge to an energy roughly halfway in between.

The method we have described is machine intensive, with large matrices to be diagonalized. This is a price that one may have to pay for dealing realistically with situations where the spatial variation cannot be reduced to dependence on a single coordinate. Our formulation, like that of Ref. 6, can be extended in principle to include the slowly varying band-bending potentials.

Use of Fourier expansion has two practical advantages relative to expansion in other sets of functions. The first is that the functions are orthogonal and complete, which means that convergence improves in a straightforward way as more functions are included in the set. The second is that if a particular plane wave is a member of the expansion set, then both its first and second derivatives are also included in the expansion set. This is not automatically true with other sets of orthogonal functions. This is important in treating coupled-equation sets where both first and second derivatives appear, as they do in envelope-function calculations where both valence and conduction bands are included in the set of nearby states.

In summary, our method makes it possible to calculate directly the optical properties of realisitic semiconductor nanostructure systems in which the carriers are confined in one or more dimensions. Quantitative comparison with experimental results are now possible and will be presented in a forthcoming publication.

[1]D. Gershoni, H. Temkin, G. J. Dolan, J. Dunsmuir, S. N. G. Chu, and M. B. Panish, Appl. Phys. Lett. **53**, 995 (1988).
[2]D. S. Citrin and Y. C. Chang, Phys. Rev. B **40**, 5507 (1989).
[3]D. S. Citrin and Y. C. Chang, J. Appl. Phys. **68**, 161 (1990).
[4]P. C. Sercel and K. J. Vahalla, Phys. Rev. B **42**, 3690 (1990).
[5]J. M. Luttinger and W. Kohn, Phys. Rev. **97**, 869 (1955).
[6]M. Altarelli, *Heterojunctions and Semiconductor Superlattices,* edited by G. Allan, G. Bastard, N. Boccara, M. Lannoo, and M. Voos (Springer-Verlag, Berlin, 1986), p. 12.
[7]D. J. Ben Daniel and C. B. Duke, Phys. Rev. **152**, 183 (1966).
[8]L. J. Sham, and M. Nakayama, Phys. Rev. B **20**, 734 (1979).
[9]S. R. White and L. J. Sham, Surf. Sci. **47**, 879 (1981).
[10]G. E. Marques and L. J. Sham, Surf. Sci. **113**, 131 (1982).
[11]G. Bastard, Phys. Rev. B **24**, 5693 (1981); **25**, 7584 (1982).
[12]M. Altarelli, in *Application of High Magnetic Fields in Semiconductors,* edited by G. Landwehr (Springer-Verlag, Berlin, 1983), p. 174.
[13]M. Altarelli, Phys. Rev. B **28**, 842 (1983).
[14]M. F. H. Schuurmans and G. W. t'Hooft, Phys. Rev. B **31**, 8041 (1985).
[15]R. Eppenga, M. F. H. Schuurmans, and S. Colak, Phys. Rev. B **36**, 1554 (1987).
[16]D. L. Smith and C. Mailhiot, Phys. Rev. B **33**, 8345 (1986).
[17]M. G. Burt, Semicond. Sci. Technol. (U.K.) **3**, 739 (1988).
[18]Richard A. Morrow and Kenneth R. Brownstein, Phys. Rev. B **30**, 678 (1984).
[19]L. C. Andreani, A. Pasquarello, and F. Bassani, Phys. Rev. B **36**, 5887 (1987).
[20]W. Potz, W. Porod, and D. K. Ferry, Phys. Rev. B **32**, 3868 (1985).
[21]G. Brozak *et al.,* Phys. Rev. Lett. **64**, 471 (1990).
[22]Qi-Gao Zhu and Herbet Kromer, Phys. Rev. B **27**, 3519 (1983).
[23]M. G. Burt, in *Band Structure Engineering in Semiconductor Microstructures,* edited by R. A. Abram and M. Jaros (Plenum, New York, 1989), p. 99.
[24]C. G. Van de Walle and R. M. Martin, J. Vac. Sci. Technol. B **3**, 125 (1985); Phys. Rev. B **34**, 5621 (1986); *ibid.* **35**, 8154 (1987); A. Baldereschi, S. Baroni, and R. Resta, Phys. Rev. Lett. **61**, 734 (1988).
[25]E. O. Kane, J. Phys. Chem. Solids **1/2**, 83 (1956).
[26]E. O. Kane, in *Handbook on Semiconductors,* edited by W. Paul (North-Holland, Amsterdam, 1982) Vol. 1, p. 193.
[27]See, for example W. E. Byerly, *An Elementary Treatise on Fourier Series and Spherical Harmonics* (Ginn and Company, Boston, 1893).
[28]G. E. Pikus and G. L. Bir, Fiz. Tverd. Tela **1**, 1624 (1959) [Sov. Phys. Solid State **1**, 1502 (1960)].
[29]Thomas B. Bahder, Phys. Rev. B **41**, 11992 (1990).
[30]D. Gershoni, J. S. Weiner, S. N. G. Chu, G. A. Baraff, J. M. Vandenberg, L. N. Pfeiffer, K. West, R. A. Logan, and T. Tanbun-Ek, Phys. Rev. Lett. **65**, 1631 (1990).
[31]*Semiconductors,* edited by O. Madelung and H. Weiss, Landolt-Börnstein, New Series, Group III, Vol. 17, Pt. A (Springer, Berlin, 1982). This reference gives effective masses, valence-band edges, spin-orbit-splitting parameters, and Luttinger parameters, which can be easily converted to the parameter set needed for the eight-band model used here.